Science Bulletin 64 (2019) 1773–1779

Contents lists available at ScienceDirect

Science Bulletin

journal homepage: www.elsevier.com/locate/scib

Science Bulletin
www.scibull.com

Article

Organic salt mediated growth of phase pure and stable all-inorganic $CsPbX_3$ (X = I, Br) perovskites for efficient photovoltaics

Taiyang Zhang [a], Yong Wang [a], Xingtao Wang [a], Min Wu [b], Wenhua Liu [a], Yixin Zhao [a,*]

[a] School of Environmental Science and Engineering, Shanghai Jiao Tong University, Shanghai 200240, China
[b] School of Environment and Energy, South China University of Technology, Guangzhou 510006, China

ARTICLE INFO

Article history:
Received 16 September 2019
Received in revised form 18 September 2019
Accepted 19 September 2019
Available online 23 September 2019

Keywords:
All-inorganic perovskite
$CsPbX_3$
Low temperature
Methylamine acetate
Solar cells

ABSTRACT

All-inorganic $CsPbX_3$ (X = I, Br) perovskites without organic component are promising for long-term stability but face main challenges of facile fabrication and phase stability. Here we discover a general organic methylamine acetate salt mediated growth method to deposit high quality phase pure and stable $CsPbX_3$ (X = I, Br) perovskite films via a novel precursor consisting of stoichiometric cesium acetate (CsAc), methylamine halide (MAX) and lead halide (PbX_2). Interestingly, these organic salts of CsAc and MAX could efficiently promote the crystallization process especially lower the crystallization temperature, but do not introduce the incorporation of organic MA cation into all-inorganic $CsPbX_3$ perovskites. These phase pure and stable $CsPbX_3$ perovskites with tunable band gaps can be fabricated into high efficiency photovoltaics. Our organic salt mediated growth of all-inorganic perovskite not only reveals the all-inorganic $CsPbX_3$ perovskite's unique crystal growth mechanism but also demonstrates their promising application for photovoltaics.

1. Introduction

The organic-inorganic hybrid perovskites-based photovoltaics with certified 23.3% efficiency record have attracted tremendous research efforts in the past years [1–9]. The hybrid perovskites' chemical instability related to potential release of volatile organic components is one of the most serious challenges for the long-term stabilities [10–13]. Therefore, the all-inorganic perovskites without volatile component become a promising alternative for perovskite solar cells. Among them, the all-inorganic $CsPbX_3$ (X = I, Br) perovskites are the most practical and promising candidates with significant efficiency progress in the past years [14–17]. Unlike the convenient fabrication of hybrid perovskite via solution chemistry, it is much more difficult to fabricate all-inorganic $CsPbX_3$ due to its high phase transformation temperature for the black phase [15,18,19]. Recently, several methods, including long-chain ammonium surfactant capping [20,21], $CsPbX_3$ quantum dots (QDs) [22,23] and acidic assisted method [15], had been reported to reduce the crystallization temperature. Since the organic surfactant used in surfactant capping method and QDs could limit their optoelectronic performance, the most popular and simple method for low temperature fabrication of $CsPbX_3$ perovskites is using the HX (X = I, Br) acid as additive or using the acidic precursor such as $HPbI_3$ or $PbI_2{\cdot}x$HI [15,24–27]. However, both the high annealing temperature and the corrosive acidic condition would limit their applications when flexible substrate or some acidic sensitive layers are used. It would be urgent to further understanding the fundamental properties especially crystal growth of all-inorganic $CsPbX_3$ perovskite.

In the previously reported manipulation of organic–inorganic hybrid perovskite crystallization, organic cation component or organic cation halide additives such as methylammonium chloride (MACl) etc. had been widely used in the deposition of high quality organic–inorganic hybrid perovskites [8,28,29]. However, to the best of our knowledge, no such organic components especially the organic cations had been reported to control the deposition of all-inorganic $CsPbX_3$ perovskites. The main concern might be the worry of forming organic–inorganic hybrid perovskite because the organic cation like formamidinium (FA^+) has been demonstrated to form a stable FA-Cs mixed cation perovskite film. In the previous organic cation hybrid perovskite, the different organic cation would also induce cation exchange in the crystallization process [24,29]. In this report, we present a general organic salt containing organic methylammonium (MA^+) cation and acetate (Ac^-) ion to cultivate the crystallization of high quality and phase pure $CsPbX_3$ (X = I, Br) perovskite films without any organic cation alloying under mild low temperature. We found that a novel

* Corresponding Author.
E-mail address: yixin.zhao@sjtu.edu.cn (Y. Zhao).

https://doi.org/10.1016/j.scib.2019.09.022
2095-9273/

precursor consisting the organic component cesium acetate (CsAc) and methylammonium halide (MAX) as alternative source for CsI with inorganic lead halide salt can realize a facile one-step deposition of high quality $CsPbX_3$ (X = I, Br) perovskite within seconds after the very fast removal of all-organic by-product of methylammonium acetate (MAAc).

2. Materials and methods

2.1. Materials

PbI_2 (99.9985%), $PbBr_2$ (99.9985%) and CsAc (99.9%) were obtained from Alfa Aesar Co., Ltd. MAI (99.99%), MABr (99.99%) and Sprio-MeOTAD (99.9%) were bought from Borun New Material Technology Co., Ltd. All the other materials were purchased from Sigma-Aldrich and used as received without any purification. The $CsPbI_3$ precursor solution was prepared by firstly dissolving 1 mmol PbI_2 and 1 mmol MAI in 2 mL dimethyl sulfoxide (DMSO) and then 1 mmol CsAc powder was added to the solution to form a 0.5 mol/L precursor solution. The precursor solution for $CsPbI_2Br$ and $CsPbBr_3$ were prepared following the similiar procedure but the DMSO solvent was changed to *N*-methyl-2-pyrrolidone (NMP) and DMSO mixture (1:9, v:v) (for $CsPbBr_3$).

2.2. Device fabrication

A ~20 nm thick compact TiO_2 layer was first coated on the pre-patterned fluorine-doped tin oxide (FTO, AGC, TEC7) by spray pyrolysis of 0.2 mol/L Ti(IV) bis(ethyl acetoacetate)-diisopropoxide 1-butanol solution at 450 °C followed by anneal at 450 °C for 1 h. After the substrates cooled down to room temperature, the substrates were then treated with UV-O_3 for 30 min before the perovskite deposition.

The $CsPbX_3$ precursor solutions were then spin coated onto the 50 °C pre-warmed c-TiO_2 coated-substrate at 2000 r/min for 30 s following by annealing at 100° for 2 min and 1 mg/mL phenyltrimethylammonium iodide (PTAI) solution treatment. A layer of hole transport material (HTM) of 0.1 mol/L spiro-MeOTAD, 0.035 mol/L bis(trifluoromethane) sulfonimide lithium salt (Li-TFSi), and 0.12 mol/L 4-tert-butylpyridine (tBP) in chlorobenzene/acetonitrile (10:1, v:v) solution were then spin coated with at 4000 r/min for 20 s after the films were cooled down to room temperature. Finally, 100-nm-thick Ag contact layer was thermally evaporated as back contact. All the process expect for the metal evaporation were processed in a drybox with relative humidity (R.H.) less than 10%.

2.3. Characterization

The absorption spectra of the $CsPbX_3$ perovskite films were recorded with a Cary-60 UV-vis spectrophotometer. The crystal structures of $CsPbX_3$ films were taken on a Shimadzu XRD-6100 diffractometer with Cu Kα radiation. The morphologies of the $CsPbX_3$ films were observed by a Bruker MultiMode Nanoscope IIIA atomic force microscope (AFM) and FEI Sirion 200 scanning electron microscope (SEM). The elementary composition of $CsPbX_3$ films were examined by a spectra were acquired with a Kratos Axis UltraDLD X-ray photoelectron spectroscopyspectrometer (XPS) using a monochromatic Al K source (1486.6 eV). The Nuclear magnetic resonance (NMR) tests were performed on a Bruker AVANCE III 600 MHz NMR Instrument using DMSO d_6 as solvent. The photocurrent density-voltage (*J-V*) curves of perovskite solar cells was measured by a Keithley 2401 source meter under simulated AM 1.5G illumination (100 mW/cm^2; Enlitech SS-F5-3A Class AAA Solar Simulator, the light intensity was calibrated by a stand Si cell before test) with a scan rate of 0.05 V/s equipmented with a non-reflective metal mask with an aperture area of 0.09 cm^2. The external quantum efficiency (EQE) curves was collected from a QE-3011 system from Enlitech. All the *J-V* and EQE test were processed in atmosphere with R.H 30%–45%.

3. Results and discussion

As illustrated in Fig. 1, the novel precursor solutions consisting of stoichiometric CsAc + MAX + PbX_2 were firstly formed by adding the stoichiometric CsAc into a pre-solved MAX + PbX_2 (X = I, Br) solution. Generally, the halide chemical composition of the final $CsPbX_3$ could be tuned by the PbX_2 + MAX. The $CsPbI_3$, $CsPbI_2Br$ and $CsPbBr_3$ perovskite films were prepared from precursor solutions of CsAc + MAI + PbI_2, CsAc + MABr + PbI_2 and CsAc + MABr + $PbBr_2$, respectively. These CsAc + MAX + PbX_2 precursor solutions can be simply one-step deposited as a smooth precursor film. The precursor films were then conveniently transformed into smooth and compact black perovskite films after a mild temperature annealing process (Fig. S1 online). The annealing temperature (~100 °C) to form black phase $CsPbI_3$ perovskite is about 200 °C lower than the temperature needed in a conventional method (~300–350 °C).

The UV-vis spectra of annealed $CsPbI_3$ film in Fig. 2a shows an absorption edge at ~716 nm (~1.73 eV), which is well consistent with previously reported black phase $CsPbI_3$ perovskite [14,15,20,21,24,25,30–32]. With the alloying of Br, the absorbance edge of the $CsPbI_2Br$ and $CsPbBr_3$ films blue shifts to ~645 nm (1.92 eV) and ~530 nm (~2.33 eV), respectively. These band gap values are well consistent with the previously reported cubic phase $CsPbI_2Br$ and $CsPbBr_3$ perovskites [14,30,33–37]. XRD patterns in Fig. 2b also suggest the successful formation of black perovskite phase $CsPbX_3$ (X = I, Br). As for the $CsPbI_3$, the characteristic γ phase perovskite peaks at ~14.2°/~14.4° and ~28.6°/~28.9° (Fig. S2 online) indicated the formation of γ-$CsPbI_3$ rather than the widely reported α-$CsPbI_3$, which is another black phase $CsPbI_3$ with slightly distorted crystal structure compared to well-known α-$CsPbI_3$ [15,18–20,26,42]. The γ-$CsPbI_3$ perovskite films exhibit much higher XRD peak intensities than the $CsPbI_2Br$ and $CsPbBr_3$ perovskite films as shown in Fig. S3 (online). For the $CsPbI_2Br$ sample, its (1 0 0) and (2 0 0) peaks shifted to ~14.6° and 29.5° due to the smaller size of Br, revealing the successfully formation of mixed halide $CsPbI_2Br$ perovskite films [30,36–38]. The peak shift became more pronounced for the tri-Br sample of $CsPbBr_3$, its (1 0 0) and (2 0 0) peaks shift to ~15.3° and 30.8°, which is well consistent with previously reported cubic $CsPbBr_3$ [33,34,39]. What's more, no impurity peaks related to δ-phase or PbX_2 residue are found in these XRD patterns. All these UV–vis spectra and XRD patterns demonstrate the successful deposition of phase pure $CsPbX_3$ perovskite films with tunable halide composition by our novel organic component mediated low temperature and non-acidic method.

SEM images in Fig. 2c–e show that all the $CsPbI_3$, $CsPbI_2Br$ and $CsPbBr_3$ samples have compact coverage. The XPS analysis was performed on these three different films deposited from precursor solutions of MAI + PbI_2, CsAc + MAI + PbI_2 and CsI + PbI_2 to determine the existence of any organic residuals. Fig. 2f–h reveal that the XPS spectra of $CsPbI_3$ perovskite film prepared from CsAc + MAI + PbI_2 precursor are almost the same as the CsI + PbI_2 sample without any organic cation components in precursor. Moreover, there is no signal belong to the N 1s found in the XPS spectra of $CsPbI_3$ sample, while the hybrid $MAPbI_3$ sample exhibits a strong N 1s peak. These results suggest the absence of MA cation alloying in the sample prepared from CsAc + MAI + PbI_2 precursor. To further exclude the possibility of organic residues including MA

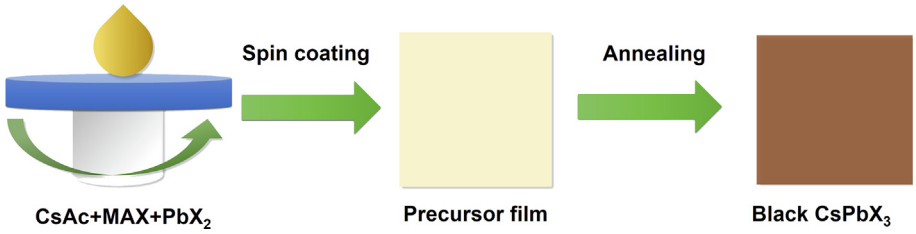

Fig. 1. (Color online) Schematic illustration of growth of black $CsPbX_3$ (X = I, Br) films using CsAc + MAX + PbX_2 precursor solutions.

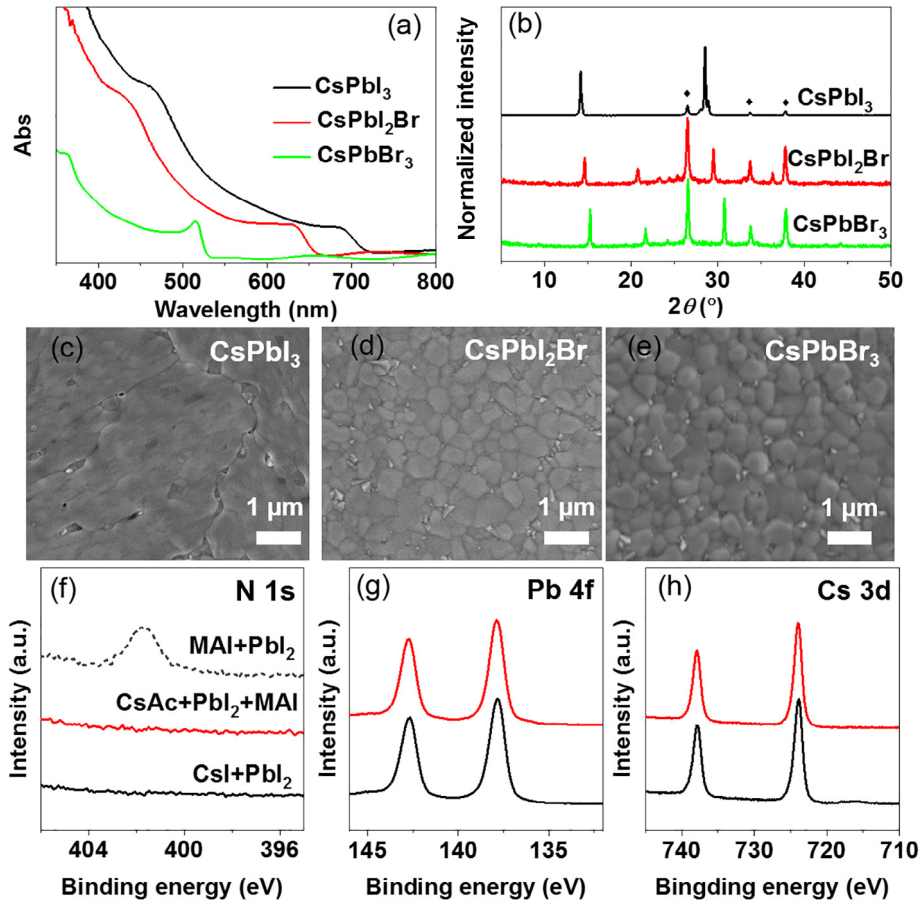

Fig. 2. (Color online) Characterization of the as-fabricated $CsPbX_3$ perovskite films. (a) UV–vis spectrums, (b) normalized XRD patterns (the raw data is shown in Fig. S3 (online)), (c-e) SEM images of $CsPbI_3$, $CsPbI_2Br$ and $CsPbBr_3$ films prepared by CsAc + MAX + PbX_2 precursors. (f) The N 1s core level XPS spectra between $MAPbI_3$ and $CsPbI_3$ films prepared by CsI + PbI_2 and CsAc + MAI + PbI_2 precursors. (g, h) Pb 4f and Cs 3d XPS spectra of $CsPbI_3$ films prepared by CsI + PbI_2 (black) and CsAc + MAI + PbI_2 (red) precursors.

cation and Ac ion, the annealed $CsPbI_3$ films were dissolved with DMSO d_6 for NMR (^1H, ^{13}C) measurements. As shown in Fig. S4 (online), there is only the DMSO d_6 solvent and H_2O peaks without no any detectable residue signal related to MA or Ac [40]. This finding is also well consistent with the facts that all these perovskite samples show characteristic XRD patterns and band gaps of phase pure $CsPbX_3$ perovskites.

All the above material characterizations show that our novel method can deposit the high quality and phase pure $CsPbX_3$ perovskites film as convenient as the previous deposition methods for inorganic–organic hybrid perovskites. It is of great significance to explore a fundamental understanding of the crystallization mechanism for the further development of this novel and general method. The $CsPbI_3$ with the highest black phase transformation temperature was selected as the model for the mechanism study. First of all, we highlight the different crystal growth process between the regular precursor of CsI + PbI_2 without organic component and our novel organic component mediated precursor of CsAc + MAI + PbI_2. The regular CsI + PbI_2 precursor films only form a pale-yellow film with an absorption peak at ~417 nm after 100 °C annealing (Fig. 3a) and its XRD patterns also show a typical δ-$CsPbI_3$ peaks at ~10°. Moreover, the SEM images in Fig. S5 (online) reveal lots of pinholes on the perovskite films, indicating the formation of a low quality δ phase $CsPbI_3$ film. This unsuccessful attempt is quite normal because the black phase transformation temperature of $CsPbI_3$ is usually up to 350 °C [15,24,37,41,42]. Therefore, we propose that the formation of black phase $CsPbI_3$ by our novel method should be ascribed to the organic component mediated crystallization procedure. The whole process seems go through the follow steps

$$CsAc + MAI + PbI_2 \rightarrow \text{Intermediate} \rightarrow CsPbI_3 + MAAc \uparrow$$

The intermediate precursor film consisting organic component of CsAc + MAI and PbI_2 must play an important role in the crystallization process. Based on the previously proposed growth mechanism for mixed FA-MA hybrid perovskites using mixed cation

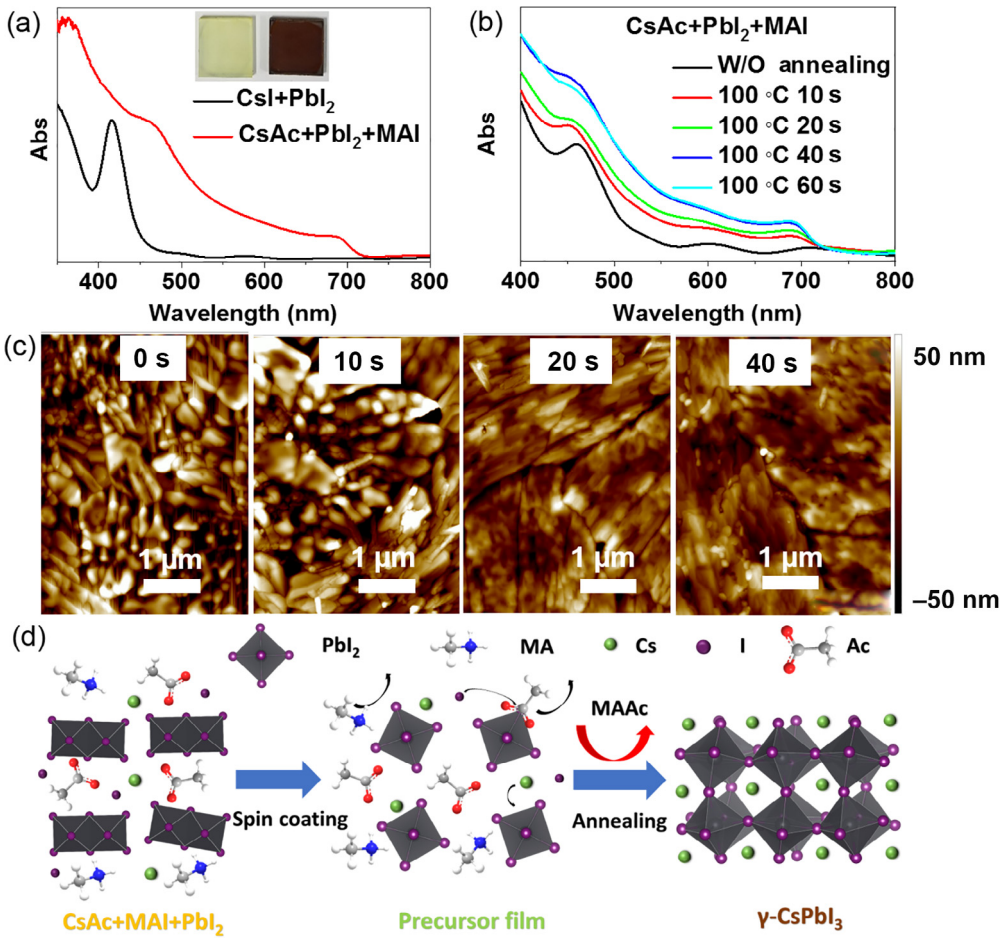

Fig. 3. (Color online) Crystallization mechanism investigation of the growth process. (a) UV-vis spectra of $CsPbI_3$ films prepared from the CsAc + MAI + PbI_2 and CsI + PbI_2 precursors, respectively. (b) UV-vis spectra evolution and (c) morphologies of CsAc + MAI + PbI_2 precursor films with different annealing duration. (d) Schematic diagram of the proposed crystallization mechanism of $CsPbI_3$ from CsAc + MAI + PbI_2 precursor.

precursor solutions [29], the $MAPbI_3$ or MA-Cs mixed perovskite may be formed initially from the CsAc + MAI + PbI_2 precursor, then the Cs^+ cation from CsAc would be incorporated by replacing the MA cation through a cation exchange reaction to obtain the final phase pure $CsPbI_3$. However, this MA-Cs cation exchange growth mechanism could be excluded based on the following fact that UV–vis absorbance blue shift related to the cation-exchange process were not observed. In contrast, an absorption edge at ~716 nm immediately appeared during annealing process as shown in Fig. 3b. There is only absorption intensity increase without any absorbance edge shift during the crystallization process. The freshly deposited CsAc + MAI + PbI_2 precursor film without annealing looks greenish, and its XRD pattern exhibits amorphous feature while the as-spun CsI + PbI_2 film shows typical δ-$CsPbI_3$ features (Fig. S6 online). The color of the CsAc + MAI + PbI_2 precursor film then immediately changes from greenish to brown after 100 °C annealing for 10 s (Fig. S7 online). Both UV–vis spectra and XRD pattern evolution suggested that the $CsPbI_3$ perovskite film is highly like to directly crystalize from precursor film of CsAc + MAI + PbI_2 via annealing. The chemical mechanism behind it might be due to the strong binding energy in all-inorganic perovskite, and previous reports has suggested that the organic cation cannot replace the Cs cation in all-inorganic $CsPbX_3$ perovskites [32,43].

Based on the above discussion, a solid intermediate precursor film consisting of $Cs_xMA_yPbI_3Ac_z$ composition with some solvent molecular would firstly form after spin coating [44]. In such intermediate precursor film, both the Cs^+ and MA^+ cations would competitively occupy the cation site of Pb-I octahedron [45] and the CH_3COO^- (Ac^-) could coordinate the surface Pb^{2+} site via Pb-CH_3COO^- bonds [46,47]. All the two proposed chemical interaction especially the later Pb-CH_3COO^- coordination could significantly decrease the symmetry thus greatly reduce the crystallinity of the precursor film. This hypothesis is consistent with both the above-mentioned amorphous feature of the precursor films and the previous mechanism study on deposition of hybrid perovskite using $Pb(Ac)_2$ precursors [44]. Moreover, this intermediated film seems to be highly unstable, and the organic components could be rapidly removed in the form of highly volatile by-product of MAAc during annealing [46,48,49]. The fast removal of MAAc by-product may lead to the dense nucleation sites, thus benefit the stabilization of initial crystallized $CsPbI_3$ with small grain size [20,24]. This hypothesized growth mechanism is supported by the morphological evolution of $CsPbI_3$ perovskite films. As measured by atomic force microscopy (AFM) in Fig. 3c, the as-deposited precursor film and the 10 s annealed precursor film show smaller size morphology while the grain size of 20 and 40 s annealed samples become as large as ~2 μm. The organic component mediated fast nucleation, distortion of Pb–I bonds and low temperature annealing may lead to the formation of γ-$CsPbI_3$, which is more phase stable at lower temperature than well-known α-$CsPbI_3$. Based on all abovementioned discussion, we illustrate the proposed crystallization process in Fig. 3d. The stoichiometric CsAc, MAI and PbI_2 dissolved in DMSO would form a Pb-I based complex colloid solution at first; a highly unstable solid intermediate precursor film consisting of Pb-I octahedron, Cs^+

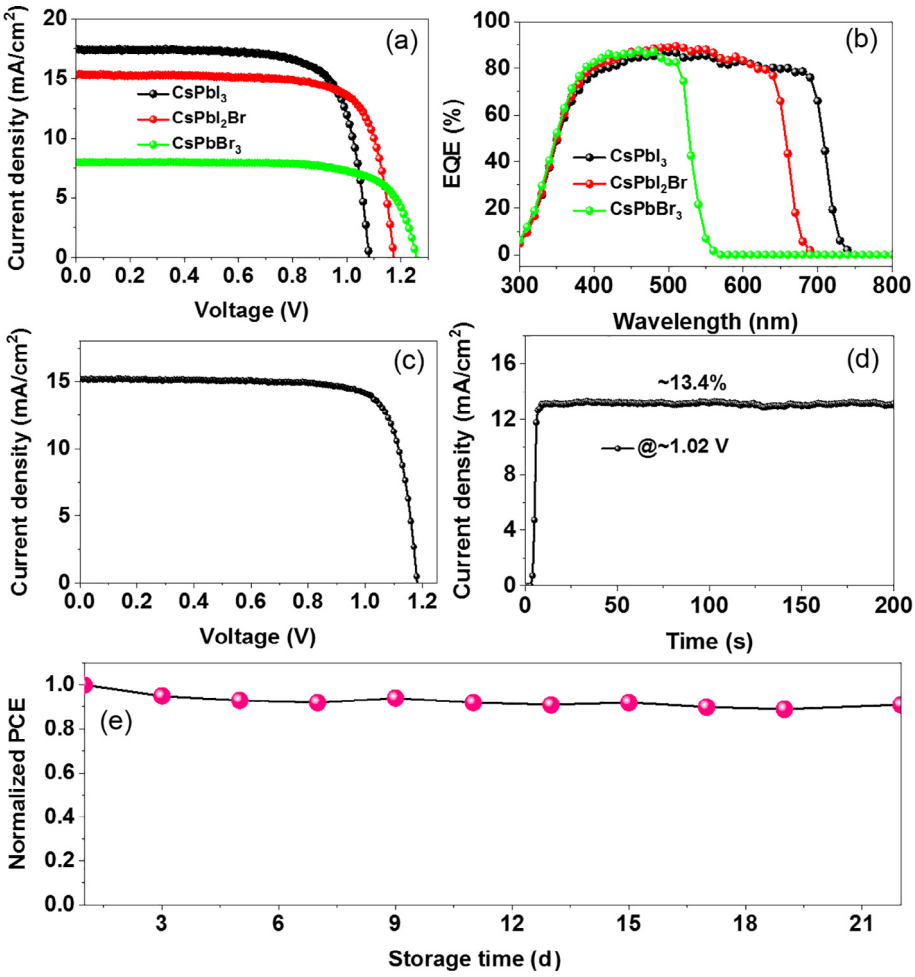

Fig. 4. (Color online) Device performance of the $CsPbX_3$ based solar cell devices. (a) *J-V* curves and (b) EQE curves of typical PTAI passivated $CsPbI_3$, $CsPbI_2Br$ and $CsPbBr_3$ solar cells; (c) *J-V* curves, (d) stable output and (e) stability test of champion PTAI passivated $CsPbI_2Br$ solar cell (the device was stored in a dark desiccator at room temperature).

and MA^+ cations and some surface Ac^- was then deposited; finally, the thermal annealing induces the crystallization of high quality $CsPbI_3$ perovskite with the rapid removal of volatile MAAc by-product from the intermediate precursor film.

All the above-mentioned characterizations demonstrated a successful deposition of high quality $CsPbX_3$ perovskite films by our novel low temperature and non-acidic method. These PTAI passivated stabilized $CsPbI_3$, $CsPbI_2Br$ and $CsPbBr_3$ perovskite films were then fabricated into solar cell device with a typical planar structure of FTO/compact-TiO_2/perovskite/Sprio-MeOTAD/Ag. As shown in Fig. 4a and Table S1 (online), the short circuit current (J_{sc}) value are ~17.3 mA/cm^2 ($CsPbI_3$), ~15.3 mA/cm^2 ($CsPbI_2Br$) and ~7.5 mA/cm^2, respectively. These values are consistent with their EQE curves in Fig. 4d. The open circuit voltage (V_{oc}) values increase from 1.08 V ($CsPbI_3$) to 1.24 V ($CsPbBr_3$) with the increasing of $CsPbX_3$ perovskite's band gap. Moreover, a champion $CsPbI_2Br$ based device reach a high efficiency of 14.23% (J_{sc} = 15.20 mA/cm^2, V_{oc} = 1.18 V and fill factor (*FF*) = 0.793, under reverse scan) with a stable out of ~ 13.4% (Fig. 4c and d). Such value is comparable with state-of-the-art efficiency achieved by other high temperature or acidic assisted methods [23,31,35,37,50]. Besides the high efficiency, the champion $CsPbI_2Br$ device also show excellent stability, it could retain more than ~90% initial efficiency after storage in dark desiccator over 3 weeks. The device stability of $CsPbI_2Br$ with larger tolerance factor is much higher than the $CsPbI_3$ samples because the chemically pure $CsPbI_3$ is intrinsically unstable under ambient conditions (Fig. S8 online). The UV–vis absorbance of δ-$CsPbI_3$ became dominant after exposed to humid air, while the $CsPbI_2Br$ films remain unchanged. Such result is well consisted with previous reports [15,30,38].

4. Conclusions

In summary, we successfully developed a general organic component mediated low temperature solution chemistry method for the deposition of high quality all-inorganic $CsPbX_3$ (X = I, Br) perovskite films. By using new precursor consisted organic components of CsAc + MAX + PbX_2, high quality $CsPbX_3$ films could be facilely one-step obtained as convenient as the hybrid perovskites. The low temperature crystallization of all-inorganic perovskite without organic cation alloy should be ascribed to the stronger binding energy in all-inorganic perovskites than hybrid ones. Finally, these PTAI passivated all-inorganic $CsPbX_3$ perovskites based solar cells exhibited high efficiencies, a $CsPbI_2Br$ based solar cell exhibited stabilized 13.4% output with high stability. Our novel method offers new choice for the low-temperature growth of high quality all-inorganic $CsPbX_3$ perovskite films for various optoelectronic applications.

Conflict of interest

The authors declare that they have no conflict of interest.

Acknowledgments

Yixin Zhao acknowledges the support of the National Natural Science Foundation of China (21777096, 51861145101) and Huoyingdong Grant (151046). Taiyang Zhang acknowledges the support of the Initiative Postdocs Supporting Program (BX20180185) and China Postdoctoral Science Foundation (2018M640387).

Author contributions

Yixin Zhao designed and directed the research. Taiyang Zhang, Yong Wang, Xingtao Wang, Min Wu, and Wenhua Liu fabricated and characterized the perovskite thin films and devices. Yixin Zhao and Taiyang Zhang analyzed the results and wrote the manuscript with inputs from all authors.

Appendix A. Supplementary materials

Supplementary materials to this article can be found online at https://doi.org/10.1016/j.scib.2019.09.022.

References

[1] Kojima A, Teshima K, Shirai Y, et al. Organometal halide perovskites as visible-light sensitizers for photovoltaic cells. J Am Chem Soc 2009;131:6050–1.
[2] Kim H-S, Lee C-R, Im J-H, et al. Lead iodide perovskite sensitized all-solid-state submicron thin film mesoscopic solar cell with efficiency exceeding 9%. Sci Rep 2012;2:1–7.
[3] Burschka J, Pellet N, Moon SJ, et al. Sequential deposition as a route to high-performance perovskite-sensitized solar cells. Nature 2013;499:316–9.
[4] Li X, Bi D, Yi C, et al. A vacuum flash-assisted solution process for high-efficiency large-area perovskite solar cells. Science 2016;353:58–62.
[5] McMeekin DP, Sadoughi G, Rehman W, et al. A mixed-cation lead mixed-halide perovskite absorber for tandem solar cells. Science 2016;351:151–5.
[6] Chen H, Ye F, Tang W, et al. A solvent- and vacuum-free route to large-area perovskite films for efficient solar modules. Nature 2017;550:92–5.
[7] Yang WS, Park BW, Jung EH, et al. Iodide management in formamidinium-lead-halide-based perovskite layers for efficient solar cells. Science 2017;356:1376–9.
[8] Jiang Q, Zhang L, Wang H, et al. Enhanced electron extraction using SnO_2 for high-efficiency planar-structure $HC(NH_2)_2PbI_3$-based perovskite solar cells. Nat Energy 2016;2:16177.
[9] Zhao Y, Zhu K. Organic-inorganic hybrid lead halide perovskites for optoelectronic and electronic applications. Chem Soc Rev 2016;45:655–89.
[10] Conings B, Drijkoningen J, Gauquelin N, et al. Intrinsic thermal instability of methylammonium lead trihalide perovskite. Adv Energy Mater 2015;5:1500477.
[11] Qin C, Matsushima T, Fujihara T, et al. Degradation mechanisms of solution-processed planar perovskite solar cells: thermally stimulated current measurement for analysis of carrier traps. Adv Mater 2015;28:466–71.
[12] Juarez-Perez EJ, Hawash Z, Raga SR, et al. Thermal degradation of $CH_3NH_3PbI_3$ perovskite into NH_3 and CH_3I gases observed by coupled thermogravimetry-mass spectrometry analysis. Energy Environ Sci 2016;9:3406–10.
[13] Domanski K, Alharbi EA, Hagfeldt A, et al. Systematic investigation of the impact of operation conditions on the degradation behaviour of perovskite solar cells. Nat Energy 2018;3:61–7.
[14] Chen H, Xiang S, Li W, et al. Inorganic perovskite solar cells: a rapidly growing field. Sol RRL 2018;2:1700188.
[15] Eperon GE, Paternò GM, Sutton RJ, et al. Inorganic caesium lead iodide perovskite solar cells. J Mater Chem A 2015;3:19688–95.
[16] Huang J, Lai M, Lin J, et al. Rich chemistry in inorganic halide perovskite nanostructures. Adv Mater 2018;30:1802856.
[17] Pan W, Wu H, Luo J, et al. $Cs_2AgBiBr_6$ single-crystal X-ray detectors with a low detection limit. Nat Photonics 2017;11:726–32.
[18] Marronnier A, Roma G, Boyer-Richard S, et al. Anharmonicity and disorder in the black phases of cesium lead iodide used for stable inorganic perovskite solar cells. ACS Nano 2018;12:3477–86.
[19] Sutton RJ, Filip MR, Haghighirad AA, et al. Cubic or orthorhombic? Revealing the crystal structure of metastable black-phase $CsPbI_3$ by theory and experiment. ACS Energy Lett 2018;3:1787–94.
[20] Fu Y, Rea MT, Chen J, et al. Selective stabilization and photophysical properties of metastable perovskite polymorphs of $CsPbI_3$ in thin films. Chem Mater 2017;29:8385–94.
[21] Wang Q, Zheng X, Deng Y, et al. Stabilizing the α-phase of $CsPbI_3$ perovskite by sulfobetaine zwitterions in one-step spin-coating films. Joule 2017;1:371–82.
[22] Swarnkar A, Marshall AR, Sanehira EM, et al. Quantum dot-induced phase stabilization of α-$CsPbI_3$ perovskite for high-efficiency photovoltaics. Science 2016;354:92–5.
[23] Bian H, Bai D, Jin Z, et al. Graded bandgap $CsPbI_2+Br_{1-x}$ perovskite solar cells with a stabilized efficiency of 14.4%. Joule 2018;2:1500–10.
[24] Zhang T, Dar MI, Li G, et al. Bication lead iodide 2D perovskite component to stabilize inorganic α- $CsPbI_3$ perovskite phase for high-efficiency solar cells. Sci Adv 2017;3. e1700841.
[25] Xiang S, Fu Z, Li W, et al. Highly air-stable carbon-based α-$CsPbI_3$ perovskite solar cells with a broadened optical spectrum. ACS Energy Lett 2018;3:1824–31.
[26] Zhao B, Jin S-F, Huang S, et al. Thermodynamically stable orthorhombic γ-$CsPbI_3$ thin films for high-performance photovoltaics. J Am Chem Soc 2018;140:11716–25.
[27] Jiang Y, Yuan J, Ni Y, et al. Reduced-dimensional α-$CsPbX_3$ perovskites for efficient and stable photovoltaics. Joule 2018;2:1356–68.
[28] Zhao Y, Zhu K. CH_3NH_3Cl-assisted one-step solution growth of $CH_3NH_3PbI_3$: structure, charge-carrier dynamics, and photovoltaic properties of perovskite solar cells. J Phys Chem C 2014;118:9412–8.
[29] Wang Z, Zhou Y, Pang S, et al. Additive-modulated evolution of $HC(NH_2)_2PbI_3$ black polymorph for mesoscopic perovskite solar cells. Chem Mater 2015;27:7149–55.
[30] Sutton RJ, Eperon GE, Miranda L, et al. Bandgap-tunable cesium lead halide perovskites with high thermal stability for efficient solar cells. Adv Energy Mater 2016;6:1502458.
[31] Chen CY, Lin HY, Chiang KM, et al. All-vacuum-deposited stoichiometrically balanced inorganic cesium lead halide perovskite solar cells with stabilized efficiency exceeding 11. Adv Mater 2017;29:1605290.
[32] Wang Y, Zhang T, Kan M, et al. Efficient α-$CsPbI_3$ photovoltaics with surface terminated organic cations. Joule 2018;2:2065–75.
[33] Rakita Y, Kedem N, Gupta S, et al. Low-temperature solution-grown cspbbr3 single crystals and their characterization. Cryst Growth Des 2016;16:5717–25.
[34] Liang J, Wang C, Wang Y, et al. All-inorganic perovskite solar cells. J Am Chem Soc 2016;138:15829–32.
[35] Liu C, Li W, Zhang C, et al. All-inorganic $CsPbI_2Br$ perovskite solar cells with high efficiency exceeding 13%. J Am Chem Soc 2018;140:3825–8.
[36] Zhang S, Wu S, Chen W, et al. Solvent engineering for efficient inverted perovskite solar cells based on inorganic $CsPbI_2Br$ light absorber. Mater Today Energy 2018;8:125–33.
[37] Wang P, Zhang X, Zhou Y, et al. Solvent-controlled growth of inorganic perovskite films in dry environment for efficient and stable solar cells. Nat Commun 2018;9:2225.
[38] Beal RE, Slotcavage DJ, Leijtens T, et al. Cesium lead halide perovskites with improved stability for tandem solar cells. J Phys Chem Lett 2016;7:746–51.
[39] Stoumpos CC, Malliakas CD, Peters JA, et al. Crystal growth of the perovskite semiconductor $CsPbBr_3$: a new material for high-energy radiation detection. Crys Growth Des 2013;13:2722–7.
[40] Gottlieb HE, Kotlyar V, Nudelman A. NMR chemical shifts of common laboratory solvents as trace impurities. J Org Chem 1997;62:7512–5.
[41] Li Z, Yang M, Park J-S, et al. Stabilizing perovskite structures by tuning tolerance factor: formation of formamidinium and cesium lead iodide solid-state alloys. Chem Mater 2015;28:284–92.
[42] Yi C, Luo J, Meloni S, et al. Entropic stabilization of mixed A-cation AbX_3 metal halide perovskites for high performance perovskite solar cells. Energy Environ Sci 2015;9:656–62.
[43] Sanehira EM, Marshall AR, Christians JA, et al. Enhanced mobility $CsPbI_3$ quantum dot arrays for record-efficiency, high-voltage photovoltaic cells. Sci Adv 2017;3:eaao4204.
[44] Hu Q, Zhao L, Wu J, et al. In situ dynamic observations of perovskite crystallisation and microstructure evolution intermediated from $[PbI_6]^{4-}$ cage nanoparticles. Nat Commun 2017;8:15688.
[45] Saliba M, Matsui T, Seo JY, et al. Cesium-containing triple cation perovskite solar cells: improved stability, reproducibility and high efficiency. Energy Environ Sci 2016;9:1989–97.
[46] Xia Y, Ran C, Chen Y, et al. Management of perovskite intermediates for highly efficient inverted planar heterojunction perovskite solar cells. J Mater Chem A 2017;5:3193–202.
[47] Zhang T, Xie L, Chen L, et al. *In situ* fabrication of highly luminescent bifunctional amino acid crosslinked 2D/3D $NH_3C_4H_9COO(CH_3NH_3PbBr_3)n$ perovskite films. Adv Funct Mater 2017;27:1603568.
[48] Zhang W, Saliba M, Moore DT, et al. Ultrasmooth organic-inorganic perovskite thin-film formation and crystallization for efficient planar heterojunction solar cells. Nat Commun 2015;6:6142.
[49] Wu Y, Xie F, Chen H, et al. Thermally stable $MAPbI_3$ perovskite solar cells with efficiency of 19.19% and area over 1 cm^2 achieved by additive engineering. Adv Mater 2017;29:1701073.
[50] Wang K, Jin Z, Liang L, et al. All-inorganic cesium lead iodide perovskite solar cells with stabilized efficiency beyond 15%. Nat Commun 2018;9:4544.

Taiyang Zhang is a postdoctoral researcher in Shanghai Jiao Tong University. He obtained his Ph.D. degree from Shanghai Jiao Tong University in 2018. His research interests focus on the synthesis of lead halide perovskite photoelectric materials, solar cell fabrications and the research of their physical and chemical nature.

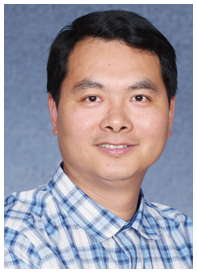

Yixin Zhao is a professor at Shanghai Jiao Tong University. He obtained his Ph.D. degree from Case Western Reserve University in 2010 followed by working as a postdoctoral fellow at Penn State University and National Renewable Energy Laboratory. His current research interests focus on perovskite solar cells, water splitting cells and functional materials for solar energy conversion and environmental remediation application.